Towards exotic nuclei via binary reaction mechanism

N. V. Antonenko,[1,2] A. K. Nasirov,[1] T. M. Shneidman,[1] and V. D. Toneev[1]

[1]*Bogoliubov Laboratory of Theoretical Physics, Joint Institute for Nuclear Research, 141980 Dubna, Moscow Region, Russia*

[2]*Institut für Theoretische Physik der Justus-Liebig-Universität, D-35392 Giessen, Germany*

Assuming a binary reaction mechanism, the yield of isotopes near the heaviest $N=Z$ neutron-deficit nucleus ^{100}Sn is studied with a microscopic transport model. The large influence of nuclear shell structure and isotope composition of the colliding nuclei on the production of exotic nuclei is demonstrated. It is shown that the reaction ^{54}Fe$+^{106}$Cd seems to be most favorable for producing primary exotic Sn isotopes which may survive if the excitation energy in the entrance reaction channel is less than about 100 MeV. In the case of large differences in the charge (mass) numbers between entrance and exit channels the light fragment yield is essentially fed from the decay of excited primary heavier fragments. The existence of optimal energies for the production of some oxygen isotopes in the binary mechanism is demonstrated for the ^{32}S$+^{197}$Au reaction. [S0556-2813(98)00404-X]

I. INTRODUCTION

Besides different applications, the production of both neutron-deficit and neutron-rich nuclei became very important for nuclear structure problems and new experiments with radioactive beams. The study of exotic doubly magic nuclei with $N=Z$ and neighboring isotopes was of a long-term interest for nuclear structure. The lightest $N=Z$ nuclei are the most stable due to the double closed shell but with increasing the atomic mass they depart from the proton drip line and become unstable against proton decay. The doubly magic ^{100}Sn nucleus having a deficit of 18 neutrons is expected to be the heaviest $N=Z$ nuclear system which is still bound. The formation of the ^{100}Sn isotope and study of its properties is quite important for further shell model development and, in particular, for the comparative study of proton-neutron interactions occupying the same orbits.

In spite of considerable efforts, experimentalists failed for a long time in attempts to produce ^{100}Sn. Only recently two groups [1,2] have synthesized this intriguing isotope using two different approaches. At GANIL [1], the reaction ^{112}Sn$+^{nat}$Ni at the intermediate energy 63 MeV/nucleon was measured, while at GSI [2], a high-energy (about 1.1 GeV/nucleon) Xe beam was used. In the latter case, the Sn nuclei were produced in high-energy fragmentation of the ^{124}Xe projectile and seven events of ^{100}Sn nuclei were observed during 277 h of beam time. The fragmentationlike reaction was employed at GANIL as well, where 11 nuclei of ^{100}Sn were identified over a period of 44 h. Taking into account the primary beam intensities, this difference in the production rate shows that the cross section for ^{100}Sn production is higher by about two orders of magnitude at intermediate energies. However, the reaction mechanisms at these two energies are quite different. In fact, high-energy fragmentation, which is considered traditionally in terms of a participant-spectator model, does not work in a whole scale at bombarding energies per nucleon of several tens of MeV. In addition, there is compelling evidence (see, for example, [3]) for simple binary reaction dynamics dominated by collective degrees of freedom. In other words, in this transitional energy range, where the reaction mechanism evolves from the dynamics of mean-field phenomena to a growing importance of two-body nucleon-nucleon interactions, projectile and target nuclei are able to largely preserve their identities and to form a damped (but not fully) dinuclear system. Nucleon exchange which occurs in this dinuclear system will be influenced by nuclear structure and, therefore, the yield of a particular isotope may depend strongly on the combination of colliding heavy ions. The aim of this paper is to study how the yield of isotopes near ^{100}Sn is sensitive to the choice of colliding nuclei and excitation energy of the dinuclear system formed. Our consideration is based on assuming a binary character of the two-nuclei interaction and on its microscopic treatment within a transport approach having relevance to the intermediate energy range of heavy-ion collisions. The method of calculation will be applied to the study of the production of different isotopes of O as well. Therefore, we may analyze the peculiarities of the production of light and heavy exotic nuclei via the binary reaction mechanism.

II. MODEL

A. Model assumptions

In the binary mechanism the interaction may be subdivided roughly into three stages: First, at the impinging stage of interaction, the colliding ions quickly lose some part of the kinetic energy of their relative motion and form a dinuclear system; then, this composite system evolves in time, exchanging nucleons, energy, and angular momentum, and this interaction terminates when the system decays into primary fragments. At the final stage the excited fragments are deexcited by particle emission, resulting in the observed reaction products. This process is very similar to deep inelastic transfer reactions taking place at lower energies (see, for example, [4–7]) but in our case a full dissipation of the relative kinetic energy is not assumed. Of course for higher energies, the division of the reaction into these stages can be considered as a first approximation and a complete study of the whole reaction dynamics is preferable. However, in order to avoid cumbersome calculations and obtain some qualita-

tive results, in this paper we will find the total dissipated energy and its partition between primary fragments using the microscopic approach [8]. Then these data will be used in the calculations of the charge (mass) distribution of reaction products.

B. Basic formalism and partition of excitation energy between primary fragments

The total Hamiltonian of a dinuclear system is written as

$$\hat{H} = \hat{H}_{\text{rel}}(\mathbf{R},\mathbf{P}) + \hat{H}_{\text{in}}(\xi) + \delta\hat{V}(\mathbf{R},\xi), \tag{1}$$

where the Hamiltonian $\hat{H}_{\text{rel}}$ describing the relative motion depends on the relative distance $\mathbf{R}$ between the centers of mass of the fragments and the conjugate momentum $\mathbf{P}$. In Eq. (1) the quantity ξ is a set of relevant intrinsic variables. The last two terms in Eq. (1) describe the internal motion of nuclei and the coupling between the collective and internal motions. The coupling term $\delta\hat{V}(\mathbf{R},\xi)$ leads to a dissipation of the kinetic energy into the energy of the internal nucleon motion.

Neglecting the residual nucleon-nucleon interaction, whose effect will be included later in the equation for the single-particle density matrix, we write the sum of the last two terms in Eq. (1) as a single-particle Hamiltonian of a dinuclear system,

$$\hat{\mathcal{H}}(\mathbf{R}(t),\xi) = \sum_{i=1}^{A_0} \left(-\frac{\hbar^2}{2m}\Delta_i + \hat{V}_P[\mathbf{r}_i - \mathbf{R}(t)] + \hat{V}_T(\mathbf{r}_i) \right), \tag{2}$$

where m is the nucleon mass, $A_0 = A_P + A_T$ is the total number of nucleons in the system, and $\hat{V}_P$ and $\hat{V}_T$ are the single-particle potentials created by the projectilelike and targetlike nuclei.

In the second quantization representation, the Hamiltonian $\hat{\mathcal{H}}(\mathbf{R}(t),\xi)$ is written as

$$\hat{\mathcal{H}}(\mathbf{R}(t),\xi) = \sum_P \widetilde{\varepsilon}_P(\mathbf{R}(t)) a_P^\dagger a_P + \sum_T \widetilde{\varepsilon}_T(\mathbf{R}(t)) a_T^\dagger a_T$$

$$+ \sum_{P \neq P'} \Lambda_{PP'}^{(T)}(\mathbf{R}(t)) a_P^\dagger a_{P'}$$

$$+ \sum_{T \neq T'} \Lambda_{TT'}^{(P)}(\mathbf{R}(t)) a_T^\dagger a_{T'}$$

$$+ \sum_{P,T} g_{PT}(\mathbf{R}(t)) (a_P^\dagger a_T + \text{H.c.}). \tag{3}$$

Here, $P \equiv (n_P, j_P, l_P, m_P)$ and $T \equiv (n_T, j_T, l_T, m_T)$ are the sets of quantum numbers characterizing the single-particle states with energies $\varepsilon_{P(T)}$ in the isolated projectilelike and targetlike nuclei, respectively. The single-particle basis is constructed from the asymptotic wave vectors of the single-particle states of the noninteracting nuclei as shown in Ref. [8]. For this basis set, the matrix elements in Eq. (3) are defined as

$$\widetilde{\varepsilon}_P(\mathbf{R}(t)) = \varepsilon_P + \langle P|V_T(\mathbf{r})|P\rangle,$$

$$\widetilde{\varepsilon}_T(\mathbf{R}(t)) = \varepsilon_T + \langle T|V_P[\mathbf{r} - \mathbf{R}(t)]|T\rangle,$$

$$\Lambda_{PP'}^{(T)}(\mathbf{R}(t)) = \langle P|V_T(\mathbf{r})|P'\rangle,$$

$$\Lambda_{TT'}^{(P)}(\mathbf{R}(t)) = \langle T|V_P[\mathbf{r} - \mathbf{R}(t)]|T'\rangle,$$

$$g_{PT}(\mathbf{R}(t)) = \frac{1}{2}\langle P|V_P[\mathbf{r} - \mathbf{R}(t)] + V_T(\mathbf{r})|T\rangle. \tag{4}$$

The nondiagonal matrix elements $\Lambda_{PP'}^{(T)}$, ($\Lambda_{TT'}^{(P)}$) generate the particle-hole transitions in the projectile (target) nucleus. The matrix elements g_{PT} are responsible for the nucleon exchange between reaction partners. Approximating the single-particle wave functions by the wave functions in the finite square well with the width depending on energy [9], these matrix elements are easily calculated. Since the trajectory calculation shows that the relative distance between the centers of the nuclei could not be less than the sum of their radii, the tails of the single-particle potentials can be considered as a perturbation disturbing the asymptotic single-particle wave functions and their energies.

With the Hamiltonian (3) the whole reaction dynamics can be studied and distributions in all observable variables can be found. To avoid a cumbersome calculation of the primary distribution of the reaction products, we use a two-step consideration. At the first stage of the reaction the average dissipated energy and its sharing between the parts of the dinuclear system are calculated with the model [8] by solving the equation for the single-particle density matrix $\widetilde{n}$,

$$i\hbar \frac{\partial \hat{\widetilde{n}}(t)}{\partial t} = [\hat{\mathcal{H}}(\mathbf{R}(t)), \hat{\widetilde{n}}(t)] - \frac{i\hbar}{\tau}[\hat{\widetilde{n}}(t) - \hat{\widetilde{n}}^{\text{eq}}(\mathbf{R}(t))]. \tag{5}$$

Here the residual interaction is taken into account in the linearized form (τ approximation), and $\widetilde{n}^{\text{eq}}(\mathbf{R}(t))$ is a local quasiequilibrium distribution, i.e., a Fermi distribution with the temperature $T(t)$. With Eq. (5) one may solve our problem in principle. Following the procedure of Ref. [8] and neglecting the dependence of single-particle potentials and levels on the charge (mass) asymmetry, one can approximately find only the first and the second moments of the mass (charge) distribution. The correct calculation of the whole mass (charge) distribution is a difficult computational problem with the formalism suggested in [8]. Therefore, at the second step of our consideration the determined excitation energy and its partition are used as inputs for the microscopic model [10], which allows us in the simple manner to calculate the charge and mass distributions formed due to the nucleon exchange between the nuclei in the dinuclear system. In the model [10] the average values of R are taken as $1.16 \times (A_P^{1/3} + A_T^{1/3})$ fm during the interaction time and only the motion in the charge (mass) asymmetry is considered; i.e., the dependence of single-particle potentials and levels on the charge (mass) asymmetry is taken into account. Our analysis shows that this two-step consideration is reasonable to estimate the yield of the exotic nuclei in the binary reaction mechanism. We found that the excitation energy E^* is almost equally shared between primary fragments in the reactions considered. For collision energies higher than 15 MeV/

nucleon, the full dissipation of the kinetic energy does not occur and the excitation energy in the system increases more slowly with $E_{\text{c.m.}}$. Thus, experimentally [3] and theoretically [8] we know that in the range 20–50 MeV/nucleon roughly half of the relative kinetic energy is transferred to the excitation energy.

C. Charge-mass distribution of primary fragments

In general, the production cross section for a primary fragment (Z,N) may be written as follows:

$$\frac{d^2\sigma}{dZdN} = 2\pi\lambdabar^2 \int_0^\infty dt \int_0^\infty dJ J\Phi(J)P_{ZN}(E_J^*,t)G(t), \quad (6)$$

where the function

$$\Phi(J) = \exp\left(-\frac{|\bar{J}-J|}{\Delta J}\right)$$

defines the angular momentum ''window'' with the width ΔJ for the given reaction and

$$G(t) = \frac{1}{\tau_0}\exp(-t/\tau_0)$$

is the lifetime distribution of the composite system characterized by some specific interaction time $\tau_0 \approx 10^{-21}$ s. The quantity $P_{ZN}(E_J^*,t)$ is the probability to find the dinuclear system at the moment t in the state with mass $A=Z+N$ and charge Z of one of the primary fragments. The excitation energy E_J^* depends on the bombarding energy E_{kin}, impact parameter (angular momentum J), and dissipation rate. In the considered energy range $E_{\text{kin}}=8$–50 MeV/nucleon the angular momentum ''window'' ΔJ for forming a particular primary isotope is rather narrow, $(10$–$20)\hbar$ (especially for low excitation energy to be of the most interest). So in the first approximation

$$\frac{d^2\sigma}{dZdN} \approx 4\pi\lambdabar^2\bar{J}\Delta J P_{ZN}(E_J^*,t_{\text{int}}), \quad (7)$$

where $t_{\text{int}} \approx 10^{-21}$ s is the average interaction time estimated for the collisions considered; $\bar{J}$ depends on E_{kin} and is smaller than the angular momentum in the grazing collision. Thus, the relative yields of the isotopes are defined by $P_{ZN}(E_J^*,t_{\text{int}})$. The value of $\bar{J}$ in Eq. (7) is defined from the trajectory calculation for each kinetic energy by using the formalism presented in Ref. [8]. This gives results which are close to the classical trajectory calculations [11].

In order to find $P_{ZN}(E_J^*,t_{\text{int}})$ characterizing the temporal evolution of the multinucleon transfer process, a dynamical model should be applied. In this work we use a version of the transport approach developed in Ref. [10]. The main advantage of this version is that the transfer process is treated on a proper microscopic footing. The consideration of proton and neutron transfers, which occur simultaneously, is based on the use of a single-particle level scheme, taking into account the isospin dependence of the single-particle energies. This is in contrast with the other dynamical approaches [4,6,12]

which studied the nucleon exchange process with smoothed (liquid-drop-like) potential energy surfaces.

On the macroscopic level, the master equation for $P_{ZN}(E_J^*,t)$ has the following form [10]:

$$\frac{d}{dt}P_{ZN}(E_J^*,t) = \Delta_{Z+1,N}^{(-,0)}P_{Z+1N}(E_J^*,t) + \Delta_{Z-1,N}^{(+,0)}P_{Z-1N}(E_J^*,t)$$

$$+ \Delta_{Z,N+1}^{(0,-)}P_{ZN+1}(E_J^*,t)$$

$$+ \Delta_{Z,N-1}^{(0,+)}P_{ZN-1}(E_J^*,t) - (\Delta_{Z,N}^{(-,0)} + \Delta_{Z,N}^{(+,0)}$$

$$+ \Delta_{Z,N}^{(0,+)} + \Delta_{Z,N}^{(0,-)})P_{ZN}(E_J^*,t), \quad (8)$$

where transition probabilities are defined as

$$\Delta_Z^{(\pm,0)} = \frac{1}{\Delta t}\sum_{P,T}|g_{PT}^Z|^2 n_{T,P}^Z(\Theta_{T,P})[1-n_{P,T}^Z(\Theta_{P,T})]$$

$$\times\frac{\sin^2[\Delta t(\widetilde{\varepsilon}_{P_Z}-\widetilde{\varepsilon}_{T_Z})/2\hbar]}{(\widetilde{\varepsilon}_{P_Z}-\widetilde{\varepsilon}_{T_Z})^2/4} \quad (9)$$

and a similar expression for $\Delta_Z^{(0,\pm)}$ with the replacement $Z \to N$. Expressions (8) and (9) are elaborated by using the Hamiltonian (3) (see Ref. [10] for details). The transition probability (9) follows Eq. (5). Here, the matrix elements g_{PT}, Eqs. (4), are taken between single-particle states of the projectilelike (P) and targetlike (T) nuclei in the dinuclear system and include both the nuclear and Coulomb (for protons) mean-field potentials. Since only the motion in the charge (mass) asymmetry is considered in this subsection, we take $R=1.16\times(A_P^{1/3}+A_T^{1/3})$ fm to calculate g_{PT} for each Z and N. In Eq. (9) we use $\Delta t=10^{-22}$ s$<t_{\text{int}}$. The single-particle occupation numbers $n_P(\Theta_P)$ and $n_T(\Theta_T)$ depend on the thermodynamical temperatures Θ_P and Θ_T in the projectilelike and targetlike nuclei, respectively.

Solving Eq. (8) with Eq. (9) at the initial conditions $P_{ZN}(E^*,0) = \delta_{Z,Z_P}\delta_{N,N_P}$ and $E^*=E^*(\bar{J},E_{\text{kin}})$, the primary isotope distributions are found for a certain interaction time t_{int}, keeping in mind relation (7). Since the collisions with small interaction times $\sim 10^{-21}$ s are mainly considered here, equal sharing of the excitation energy between the parts of the dinuclear system is used in accordance with the results of the previous subsection.

D. Secondary distribution

If the primary isotope distribution is known, the secondary (observable) isotope distributions can be estimated by applying the statistical decay model to every excited primary fragment [13]. In binary reactions one can expect the competition of two processes determining the final yield of the exotic isotopes. With increasing excitation energy the primary yield of the exotic nuclei increases but the surviving probability of these isotopes may be reduced in the subsequent deexcitation process. However, the deexcitation process takes two opposite roles. On the one hand, it reduces the multiplicity of the primary exotic isotopes obtained. On the other hand, it can increase the final yield of the exotic nuclei due to the decay of heavier primary nuclei which are not
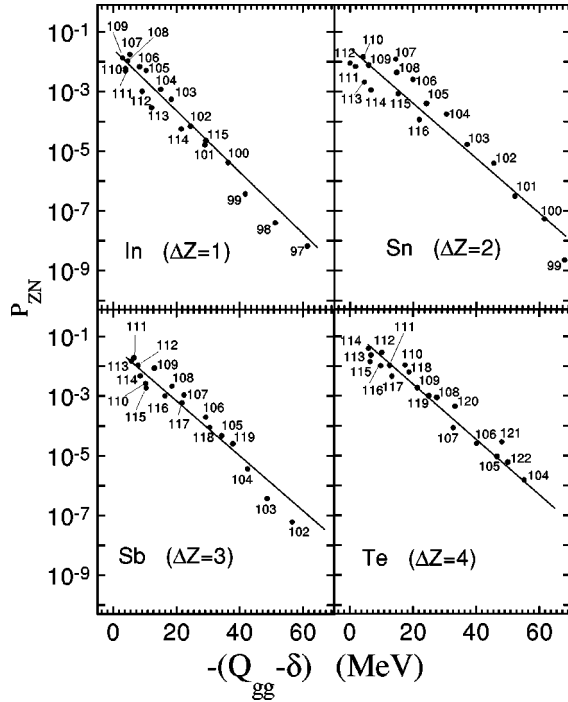
FIG. 1. The calculated Q_{gg} systematics of primary yields for In, Sn, Sb, and Te isotopes (points) from ^{58}Ni$+^{106}$Cd collision with the initial temperature $\Theta = 3.5$ MeV. The solid lines are drawn to guide the eye.

FIG. 2. The same as in Fig. 1, but for $\Theta = 2.0$ MeV.

exotic. The last effect can be called the feeding effect. Therefore, for the production of exotic nuclei, the choice of the colliding nuclei and kinetic energy should supply the optimal relationship between the primary isotope distribution and deexcitation process.

III. RESULTS AND DISCUSSION

A. Production of exotic light isotopes of Sn

Let us start from a discussion of the primary yield of exotic isotopes of Sn in different reactions. In Figs. 1 and 2 the calculated primary yield of isotopes produced in the ^{58}Ni$+^{106}$Cd reaction, which is considered as one of the most promising combinations for ^{100}Sn production, are presented in the form of Q_{gg} systematics (δ is the so-called "nonpairing" energy correction) [7]. The calculation results are given for the equilibrium initial temperatures $\Theta = 3.5$ and 2.0 MeV which correspond to the excitation energies 200 and 65 MeV, respectively. It is seen that the isotope yields follow Q_{gg} systematics in both cases, and so the shell structure effects [inherent to the transition probabilities (9)] at least survive until the temperature is as high as 3.5 MeV. Ranging over six to eight orders of magnitude, P_{ZN} at the given temperature can be approximated rather well by a single straight line (in the logarithmic scale). However, the slope of this line does not coincide with the initial temperature T and even does not scale with T: Slopes in Figs. 1 and 2 differ by about 30%. One should note that full thermodynamical equilibrium has not been assumed in the microscopic transport model. Therefore, the Q_{gg} systematics cannot be considered as evidence in favor of full thermodynamical equilibrium in the evolution of a dinuclear system. Nevertheless, the Q_{gg} sys-
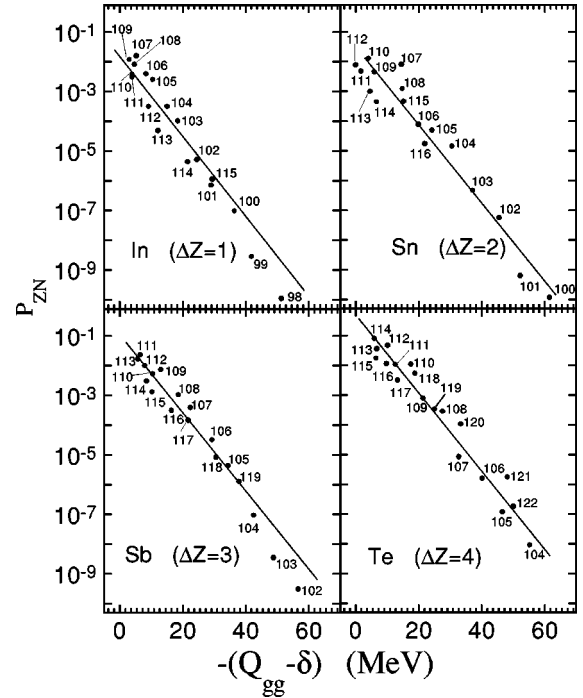
tematics seems to be a useful working method for estimating the yield of isotopes far away from the line of stability.

The primary yield of exotic nuclei may be very sensitive to the combination of colliding ions. As demonstrated in Fig. 3, the use of an ^{54}Fe target instead of ^{56}Fe in the reaction with a ^{106}Cd beam increases the primary yield of neutron-deficit Sn isotopes by an order of magnitude. The yield increases rapidly with the excitation energy and this growth is more pronounced for ^{100}Sn than for heavier tin isotopes. Note that subsequent deexcitation may suppress the primary isotope yield at high E^* (see below).

Similar trends are seen from the excitation functions for various reactions presented in Fig. 4. In addition, the results for ^{64}Zn$+^{106}$Cd and ^{40}Ca$+^{106}$Cd collisions turned out to be close numerically to those for ^{58}Ni$+^{112}$Sn and ^{58}Ni$+^{106}$Cd
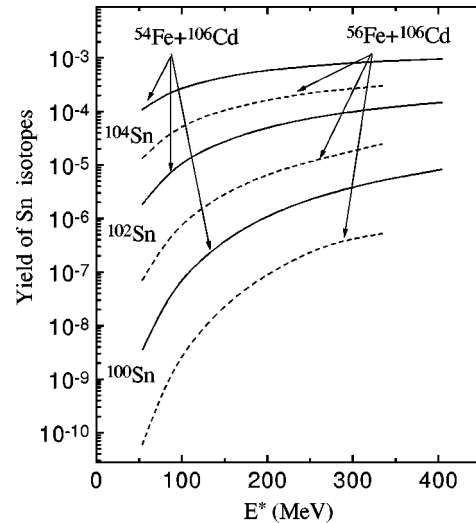

FIG. 3. The excitation functions of Sn isotopes from ^{54}Fe$+^{106}$Cd (solid lines) and ^{56}Fe$+^{106}$Cd (dashed lines).
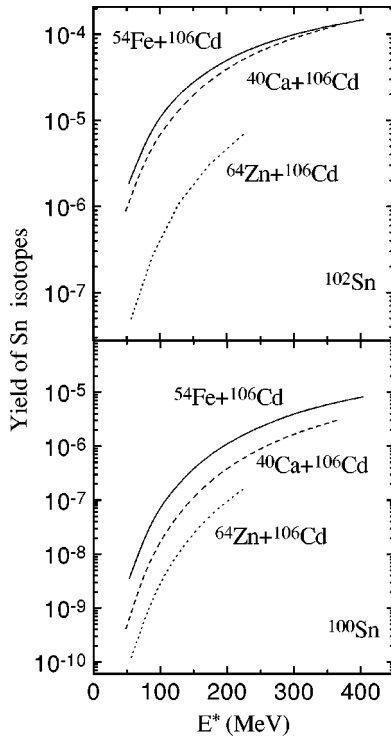
FIG. 4. The excitation energy dependence of ^{102}Sn (upper part) and ^{100}Sn (lower part) for three composite systems: ^{54}Fe+^{106}Cd (solid lines), ^{40}Ca+^{106}Cd (dashed lines), and ^{64}Zn+^{106}Cd (dotted lines).
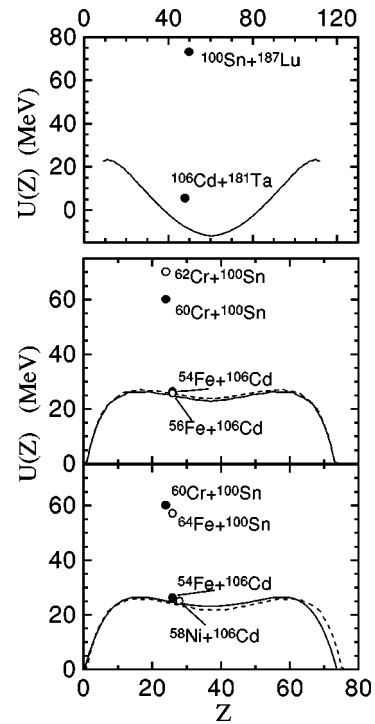

FIG. 5. The charge-asymmetry dependence of a smoothed part of potential energy in N/Z equilibrium for the following systems: ^{54}Fe+^{106}Cd (solid lines), ^{56}Fe+^{106}Cd (dashed line, middle part), ^{58}Ni+^{106}Cd (dashed line, lower part), and ^{181}Ta+^{106}Cd (solid line, upper part). The points correspond to the system energy in the entrance channel and to that in the final state with the ^{100}Sn isotope.

(see also Figs. 1 and 2) reactions. Among all the cases considered, the ^{54}Fe+^{106}Cd reaction, which has the smallest neutron number in the entrance channel, seems to give the largest primary yield of ^{100}Sn.

The reasons for a preference of the ^{54}Fe+^{106}Cd reaction are illustrated in Fig. 5, where the smoothed driving potential $U(Z)$ defined by

$$U(Z) = B_1 + B_2 + U_{12}(R_m) - B_0 \qquad (10)$$

is shown. Here B_1 and B_2 are the liquid drop binding energies of the nuclei in the dinuclear system, and $U_{12}(R_m)$ is the value of the nucleus-nucleus potential at distance $R_m = R_1 + R_2 + 0.5$ fm [14]. The calculated results are reduced to the binding energy B_0 of the compound nucleus. Since the difference between the moment of inertia of the dinuclear system including ^{100}Sn as one of the fragments and the moment of inertia of the initial dinuclear system is very small in the reactions considered, the driving potential can be taken for zero angular momentum to analyze the energy thresholds for production of ^{100}Sn. For the reactions ^{54}Fe+^{106}Cd and ^{56}Fe+^{106}Cd, $U(Z)$ is practically the same but the energy barrier in the exit channel corresponding to ^{100}Sn is higher by ~ 10 MeV in the last case, which dramatically reduces the ^{100}Sn yield. Comparing reactions on ^{54}Fe and ^{58}Ni targets (lower part of Fig. 5), one can see that there is no essential difference in the energy barriers for producing ^{100}Sn. However, the driving force $|dU(Z)/dZ|$ near the entrance point is slightly larger for the case of the ^{58}Ni target and this system moves towards a smaller charge asymmetry with a higher probability. Both arguments, high-energy barrier and large driving force, are valid for ^{181}Ta+^{106}Cd colli-

sions (upper part of Fig. 5), and so it is hardly ever possible to produce ^{100}Sn in this reaction.

Figure 6 shows how the primary yield is modified by particle emission. It was assumed that the excitation energy E^* is partitioned equally between primary fragments. Such a partition results from the analysis of experimental data for
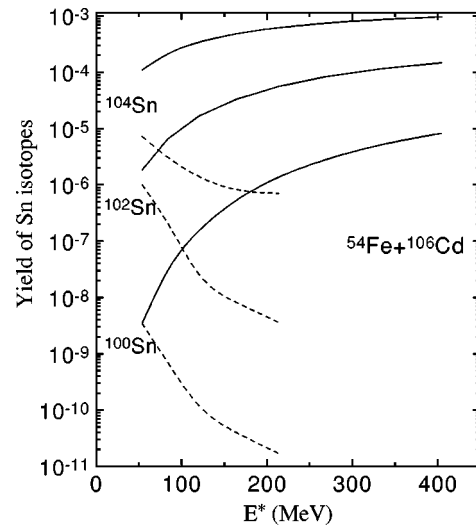

FIG. 6. The excitation functions of Sn isotopes from the ^{54}Fe+^{106}Cd reaction. The primary yield is shown by solid lines, and the dashed lines take into account the depletion due to the deexcitation process. An equal partition of the excitation energy is used in the calculations.
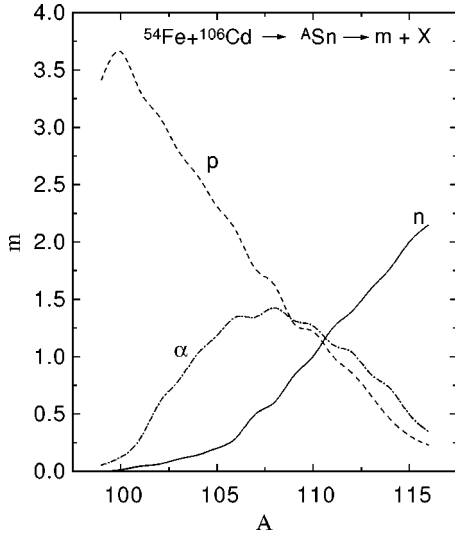
FIG. 7. Average multiplicity of particles (neutrons, protons, and α particles) emitted from the given primary Sn isotope produced in the $^{54}Fe+^{106}Cd$ reaction for an initial excitation energy $E^*=80$ MeV.

FIG. 8. The primary (lower part) and secondary (upper part) yields of the ^{15}O (dashed line), ^{19}O (dotted line), and ^{21}O (solid line) nuclei as a function of kinetic energy in the $^{32}S+^{197}Au$ reaction. The experimental points are taken from [17].

peripheral collisions [15] and is reproduced qualitatively in our calculations [8]. It is noteworthy that such an energy sharing is in conflict with the hypotheses of thermodynamical equilibrium, but it is in agreement with the particle-hole nature of the interactions in the dinuclear system. Experimental data [16] show that, for very short interaction times in the deep inelastic transfer reactions, a large part of the excitation energy belongs to the light fragments. With increasing interaction time, the sharing of the excitation energy is driven towards the thermal equilibrium limit but does not reach it. The isotope distribution of the deexcited fragments is expected to be sensitive to the excitation energy sharing. As is seen in Fig. 6, the deexcitation process changes the situation drastically: Only neutron-deficit nuclei with $E^*<100$ MeV may survive. The practical interpretation of this is that only very peripheral collisions or collisions in which the main part of the excitation energy is in the light fragment will be effective for producing these Sn isotopes. As shown in Fig. 7, the excited neutron-deficit Sn isotopes decay mainly by charged particle emission. Thus, direct use of the Sn beam may not be the most effective way to reach the ^{100}Sn isotope. The last argument may turn out to be important for production of this isotope in the high-energy fragmentation method [2], as well.

B. Production of oxygen isotopes

The example considered above concerns the production of exotic nuclei in reactions with a charge number of projectile (target) close to the charge number of the exotic nucleus under question. In these reactions the deexcitation process depletes the yield of the exotic nucleus. Let us now consider the production of oxygen isotopes in the reaction $^{32}S+^{197}Au$. In this case the light nucleus in the initial dinuclear system is far from O and the production of the O isotopes follows a long path of nucleon transfers. As a result, a large number of intermediate nuclei between S and O is
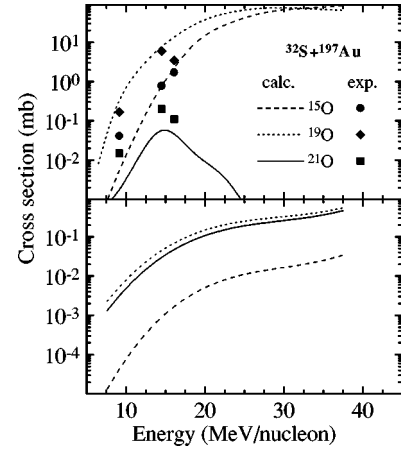
primarily produced. The decays of these nuclei in the deexcitation process can give rise to the O isotopes which are of interest to us. Therefore, in the $^{32}S+^{197}Au$ reaction one can expect a large feeding effect for the O isotopes due to the deexcitation of the primary nuclei.

In Fig. 8 the primary yield of the ^{15}O, ^{19}O, and ^{21}O isotopes is shown as a function of E_{kin}. This yield quickly grows with E_{kin} up to the value of 20 MeV/nucleon and then some saturation occurs. In accordance with Q_{gg} systematics, the primary yield of ^{15}O is smaller than yields of ^{19}O and ^{21}O. The deexcitation process strongly influences the excitation functions (Fig. 8). The calculated excitation functions are in reasonable agreement with the experiment [17]. Because of emission of charged particles and neutrons from nuclei heavier than the given O isotopes, its secondary yield increases as compared to the primary one. This feeding effect increases the yield of ^{15}O by about two orders of magnitude as compared to the primary yield. As is seen in Fig. 8 the primary yields of ^{19}O and ^{21}O are close to each other. The feeding effect increases the yield of ^{19}O much more than ^{21}O. In addition, the yield of the neutron-rich isotopes such as ^{21}O is depleted due to the neutron emission. For heavy isotopes, for example ^{21}O, the secondary excitation function may have a maximum at a certain energy. Therefore, there is an optimal colliding energy for the production of the given neutron-rich isotope. The yields of ^{15}O and ^{19}O isotopes reach saturation at an energy of about 20 MeV/nucleon. At lower values of E_{kin} the O yield is small due to the small primary yield and weak influence of the feeding effect. At higher energies the deexcitation process starts to deplete the O yield because the centers of the charge and mass distributions of the reaction products are shifted to the lighter nuclei. In this case the saturation regime is reached for the neutron-deficit isotopes, while the yield of the neutron isotopes as ^{21}O started to decrease. The optimal energy for producing light exotic nuclei in binary reactions seems to be between 15 and 25 MeV/nucleon. The most interesting results to be inferred from Fig. 8 are the feeding effect for the reactions in which the exit channel is far from the entrance

channel and the existence of optimal colliding energies for the production of some isotopes.

IV. SUMMARY

In conclusion note that the binary mechanism is realized in the context of the microscopic transport model and that the yield of exotic nuclei depends essentially on the shell structure of the nuclear partners in the entrance and exit channels. Production of the given isotope may be optimized by an appropriate choice of colliding ions. In particular, for producing neutron-deficit ^{100}Sn, the reaction ^{54}Fe$+^{106}$Cd seems to be the most effective in comparison with the reactions ^{56}Fe$+^{106}$Cd, ^{64}Zn$+^{106}$Cd, ^{58}Ni$+^{106}$Cd, ^{58}Ni$+^{112}$Sn, and ^{40}Ca$+^{106}$Cd due to a comparatively low-energy barrier and small charge drift towards N/Z equilibrium. Only primary neutron-deficit isotopes with an excitation energy less than ~ 100 MeV may survive in strong competition with charged particle emission, which puts additional limits on angular momenta contributing to an observable yield of the given isotope.

For the reactions with a considerable difference in charge (mass) numbers between entrance and exit channels, the feeding effect is important in the yield of some exotic nuclei. Because of the emission of a charged particle from nuclei heavier than the isotope studied, the production of some exotic isotopes is possible. For these reactions, there exists the optimal colliding energy for the production of a specific isotope.

For more detailed predictions, consideration of all stages (dissipation of the excitation energy, its sharing, and nucleon transfer) of the interaction should be self-consistently included in the model. This work is in progress, now based on [4]. Further model development needs also some experimental support. In addition to isotope, angular, and momentum distributions to control the dissipation process, knowledge of the excitation functions and energy dependence of the isotope dispersion is of great interest for the reactions under discussion.

ACKNOWLEDGMENTS

[1] M. Lewitowicz *et al.*, Phys. Lett. B **332**, 20 (1994).

[2] R. Schneider *et al.*, Z. Phys. A **348**, 241 (1994).

[3] W. U. Schröder, in *Proceedings of the International School-Seminar on Heavy Ion Physics*, Dubna, 1993, edited by Yu. Oganessian and R. Kalpakchieva (JINR, Dubna, 1994), p. 166.

[4] R. Schmidt, V. D. Toneev, and G. Wolshin, Nucl. Phys. **A311**, 247 (1978).

[5] W. U. Schröder and J. R. Huizenga, in *Treatise on Heavy-Ion Science*, edited by D. A. Bromley (Plenum Press, New York, 1984), Vol. 2, p. 115.

[6] H. Feldmeier, Rep. Prog. Phys. **50**, 915 (1987).

[7] V. V. Volkov, Phys. Rep. **44**, 93 (1978); in *Treatise on Heavy-Ion Science* [5], Vol. 8, p. 101.

[8] G. G. Adamian, A. K. Nasirov, N. V. Antonenko, and R. V. Jolos, Phys. Part. Nuclei **25**, 583 (1994); G. G. Adamian, R. V. Jolos, and A. K. Nasirov, Z. Phys. A **347**, 203 (1994); G. G. Adamian, R. V. Jolos, A. K. Nasirov, and A. I. Muminov, Phys. Rev. C **53**, 871 (1996); **56**, 373 (1997).

[9] G. G. Adamian, R. V. Jolos, and A. K. Nasirov, Sov. J. Nucl. Phys. **55**, 660 (1992); G. G. Adamian, N. V. Antonenko, R. V. Jolos, and A. K. Nasirov, Nucl. Phys. **A551**, 321 (1993).

[10] N. V. Antonenko and R. V. Jolos, Z. Phys. A **338**, 423 (1991); N. V. Antonenko, E. A. Cherepanov, A. S. Iljinov, and M. V. Mebel, J. Alloys Compd. **213/214**, 460 (1994).

[11] R. Schmidt, Part. Nuclei **13**, 1203 (1982).

[12] J. Randrup, Nucl. Phys. **A383**, 468 (1982); **A474**, 219 (1987).

[13] V. S. Barashenkov and V. D. Toneev, *High Energy Interaction of Particles and Nuclei with Atomic Nuclei* (Atomizdat, Moscow, 1972).

[14] G. G. Adamian, N. V. Antonenko, R. V. Jolos, S. P. Ivanova, and O. I. Melnikova, Int. J. Mod. Phys. E **5**, 191 (1996).

[15] K. Kwiatkowski, R. Planeta, S. H. Zhou, V. E. Viola, H. Breuer, M. A. McMahan, and A. C. Mignerey, Phys. Rev. C **41**, 958 (1990); **44**, 390 (1991).

[16] J. Toke and W. U. Schröder, Annu. Rev. Nucl. Part. Sci. **42**, 401 (1992).

[17] O. B. Tarasov *et al.*, JINR Report No. 2[82]-97, 1997 47; GANIL Report No. P 97 31, 1997.